AIAA SciTech
4-8 January 2016, San Diego, California, USA
57th AIAA/ASCE/AHS/ASC Structures, Structural Dynamics, and Materials Conference

AIAA 2016-1716

Thermo-Structural Design of the Hexafly-INT Experimental Flight Test Vehicle (EFTV) and Experimental Service Module (ESM)

Valerio Carandente[1] and Roberto Scigliano[2]
Italian Aerospace Research Centre (CIRA), Via Maiorise snc, Capua, Italy, 81043

Over the last years, innovative concepts of civil high-speed transportation vehicles were proposed. These vehicles have a strong potential to increase the cruise range efficiency at high Mach numbers, thanks to efficient propulsion units combined with high-lifting vehicle concepts. Nonetheless, performing a flight test will be the only and ultimate proof to demonstrate the technical feasibility of these new promising concepts and would result into a major breakthrough in high-speed flight. In this framework the Hexafly-INT project has the scope to test in free-flight conditions an innovative gliding vehicle with several breakthrough technologies on-board. This work describes both the thermo-structural design process of the Hexafly-INT Experimental Flight Test Vehicle, namely EFTV, and of the Experimental Service Module, namely ESM. The paper will present results of a Finite Element thermal analysis, performed in the most critical phases along the flight trajectory in order to drive a preliminary material selection.

I. Introduction

OVER the last years, innovative concepts of civil high-speed transportation vehicles and the development of related technologies were proposed in European Commission co-funded projects like ATLLAS, LAPCAT and HEXAFLY[1,2,3]. These vehicles have a strong potential to increase the cruise range efficiency at high Mach numbers, thanks to efficient propulsion units combined with high-lifting vehicle concepts[4,5].

Nonetheless, performing a flight test will be the only and ultimate proof to demonstrate the technical feasibility of these new promising concepts and technologies and would result into a major breakthrough in high-speed flight. At present, the expected performances are usually demonstrated by numerical simulations and only partly by experimental tests. As high-speed wind tunnels are intrinsically limited in size, it is nearly impossible to completely fit even modest vehicle planform into a tunnel. Though numerical simulations are less restrictive in geometrical size, they struggle however with accumulated uncertainties in their modelling, making predictions doubtful without inflight validation. As a consequence, the obtained technology developments are now limited to a Technology Readiness Level (TRL) equal to 4 (components validated in laboratory).

The HEXAFLY-INT project aims at the free flight testing of an innovative high-speed vehicle with several breakthrough technologies on board[6,7]. This approach will create the basis to gradually increase the TRL.

The vehicle design, manufacturing, assembly and verification will be the main driver and challenge in this project, in combination with a mission tuned sounding rocket. The prime objectives of this free-flying high-speed cruise vehicle shall aim at[4]:
- a conceptual design demonstrating a high aerodynamic efficiency at cruise conditions with a high volumetric efficiency;
- a positive aerodynamic balance at a controlled cruise Mach numbers from 7 to 8;
- a good gliding performance from Mach 7 to 2;
- an optimal use of advanced high-temperature resistant materials and/or structures.

The main flight sequence profile and mission events are shown in Fig. 1 and listed in Table 1[5,8,9]. In particular, from Fig. 1 and Table 1, it is evident that the separation between the launcher and the whole vehicle, consisting of the Experimental Flight Test Vehicle (EFTV) and the Experimental Support Module (ESM), occurs around the apogee of the sounding rocket parabolic trajectory. Then, in the first part of the descent, the vehicle attitude is controlled by the

---

[1] Research Engineer, Thermal Structures and Thermal Control Technologies and Design, v.carandente@cira.it.

[2] Research Engineer, Thermal Structures and Thermal Control Technologies and Design, r.scigliano@cira.it.

1
American Institute of Aeronautics and Astronautics

Cold Gas System (CGS) included in the ESM. When the dynamic pressure along the flight path is large enough to guarantee the aerodynamic manoeuvrability of the EFTV, the ESM is released. Finally, after a pull out manoeuvre, the EFTV starts its aerodynamically controlled cruise flight. The analysed EFTV and ESM configurations are shown in Fig. 2[8].

In the present work the methodology and the implementation of tools for thermal analysis of the EFTV and of the ESM is presented[9]. Thermal analyses are performed on the basis of the trajectory provided by Gas Dynamics Limited (GDL) and of the structural layout developed by Tecnosistem Engineering & Technology (TET).
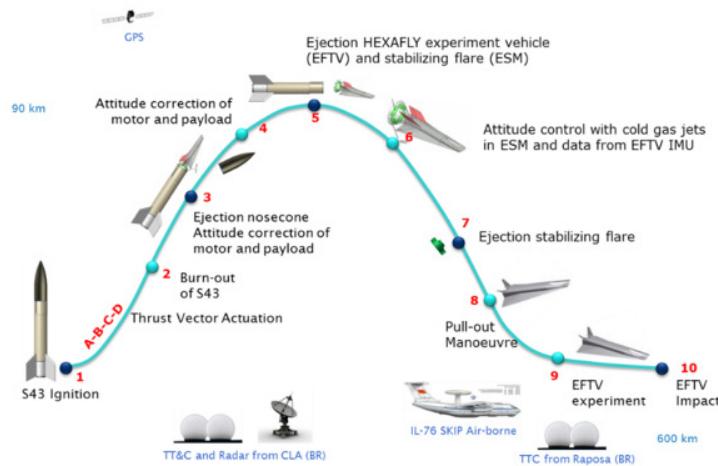

Figure 1. Flight sequence profile[5].

Table 1. Flight sequence events[5].

#	Flight Event
1-2	Propelled ascent
2	Motor burnout
3	Nose-cone ejection
4	L/V alignment
5	ESM/EFTV release
6	Attitude control by CGS in the ESM
7	Ejection of ESM
8	Pull-out manoeuvre
9	Controlled flight
10	Impact

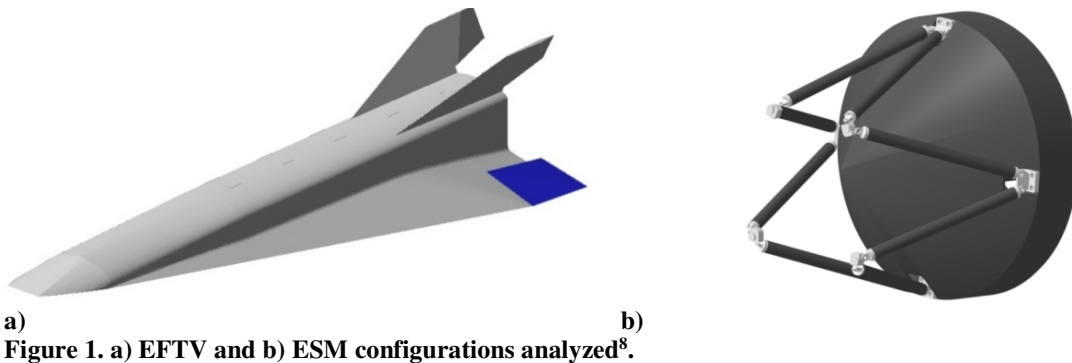

a)   b)

Figure 1. a) EFTV and b) ESM configurations analyzed[8].

II. Flight Trajectory

Flight mechanic analyses have been performed by GDL in different mission segments. In the present paper, the flight trajectory of the entire vehicle, consisting of the ESM attached to the EFTV, has been considered from the trajectory apogee up to an altitude of 50 km during the descent leg (see Fig. 3). Then, a second segment, referred to the EFTV after the separation from ESM, has been analyzed (see Fig. 4). In particular, Fig. 3a and Fig. 4a provide the time histories of altitude and velocity during descent, starting from the trajectory apogee and the ESM release, respectively. The convective heat transfer coefficient profiles at the EFTV stagnation point, provided in non-dimensional form as input to the thermal analysis hereinafter discussed, are shown in Fig. 3b and in Fig. 4b for the two mission phases. These profiles have been derived from the corresponding convective heat fluxes, estimated by means of the Tauber's[10] relationship throughout the descent flight. The EFTV nose leading edge radius is 2 mm and the aerothermal loading conditions refer to radiatively cooled walls with a surface emissivity of 0.4.

2

American Institute of Aeronautics and Astronautics
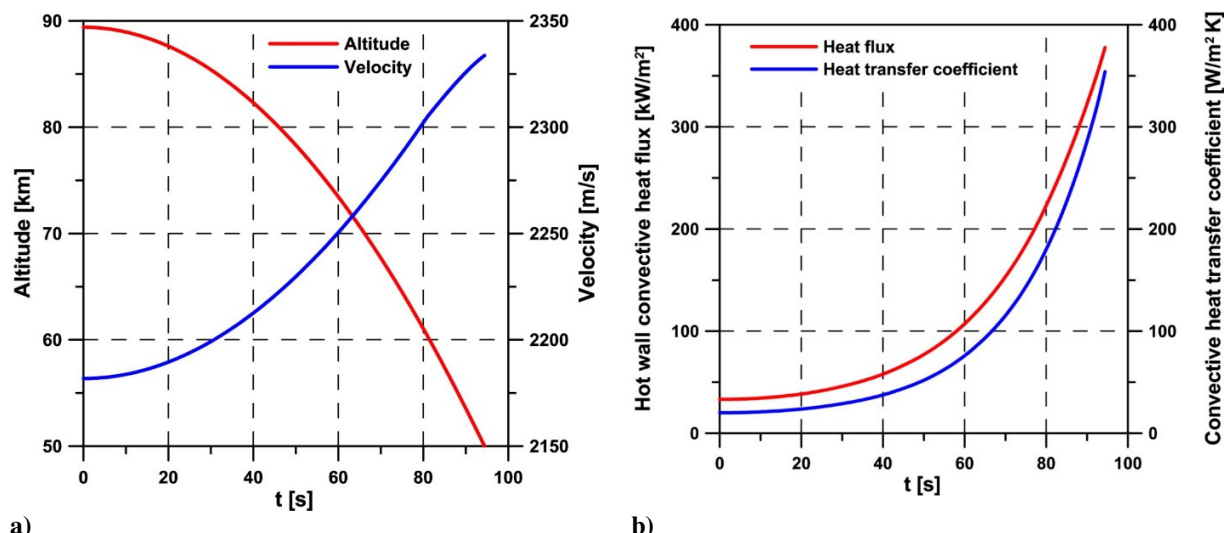
a)   b)

Figure 3. Flight trajectory for the entire vehicle (EFTV+ESM) from the apogee to 50 km altitude. a) Altitude and velocity profiles, b) convective heat flux on the EFTV stagnation point and corresponding convective heat transfer coefficient.
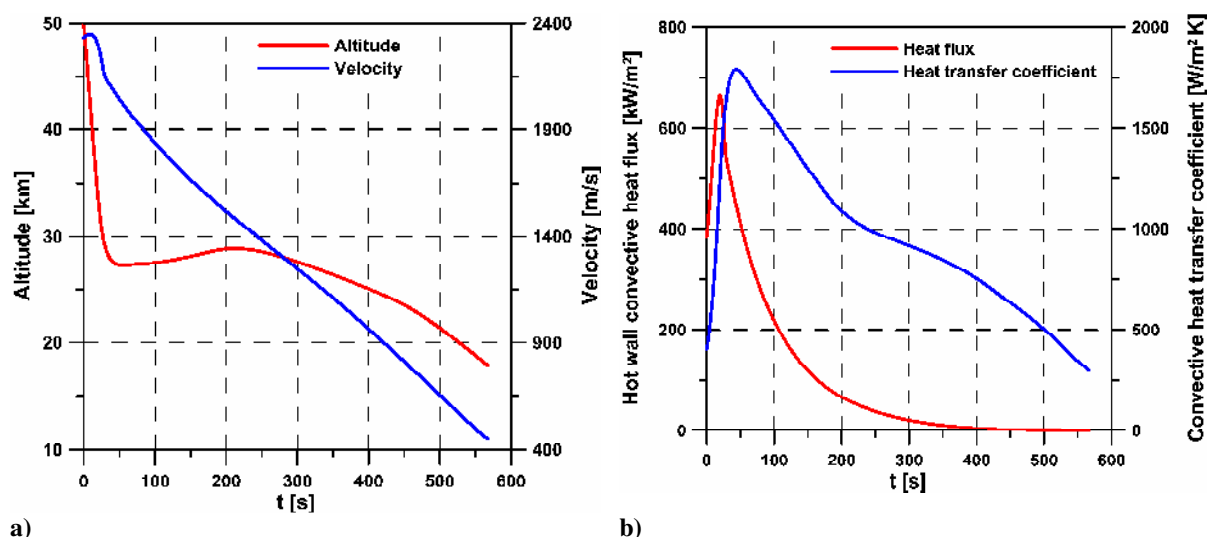
a)   b)

Figure 4. Flight trajectory for the EFTV below 50 km altitude. a) Altitude and velocity profiles, b) convective heat flux at the EFTV stagnation point and corresponding convective heat transfer coefficient.

III.   Candidate Materials

Different classes of materials have been preliminarily selected and analyzed for the EFTV and the ESM structures, namely: titanium alloy, aluminium, copper, C/C-SiC and zirconia for surface coatings. This should give a first estimation of the characteristic behavior of potential materials along the analyzed flight trajectory.

Titanium alloys exhibit a unique combination of mechanical and physical properties and corrosion resistance which have made them desirable for critical, demanding aerospace applications, also in high temperatures conditions. Aluminium is widely used in the aerospace field for its excellent strength to weight ratio. Copper is employed in this case as a heat sink to accommodate the thermal energy in some critical components (e.g. nose, leading edges). C/C-SiC developed at DLR[11] and tested in different high temperatures applications (e.g. HIFiRE and SHEFEX) is considered for ailerons and for the final part of the wing leading edge. A zirconia coating layer has been also considered to protect metallic components, increasing their surface emissivity and confining the larger temperatures on the coating itself.

3

American Institute of Aeronautics and Astronautics

Thermal and mechanical properties of titanium alloy and zirconia coating have been provided by TsAGI, Tsentralniy Aerogidrodinamicheskiy Institut (Central Aerohydrodynamic Institute), which is in charge of the system manufacturing.

In particular, the assumptions on the materials reported in Table 2 have been carried out on the ESM components shown in Fig. 5.

Table 1. Preliminarily material assignment for the main ESM structural components

ESM		
External Coating	**Rods**	**Internal Structure**
Zirconia	Titanium Alloy	Aluminium
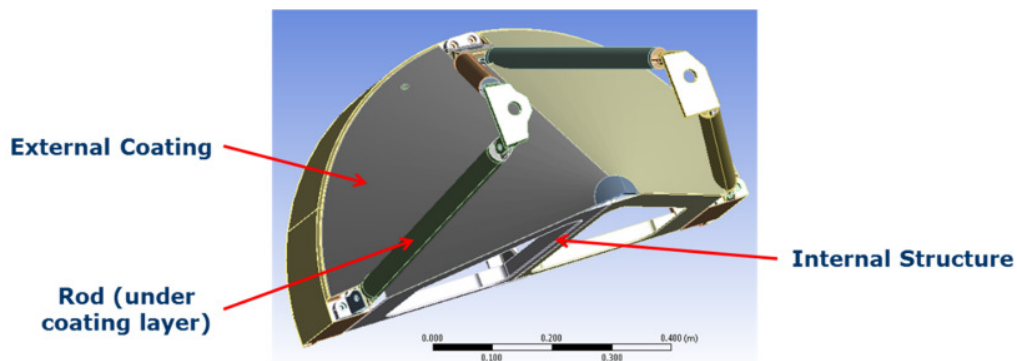
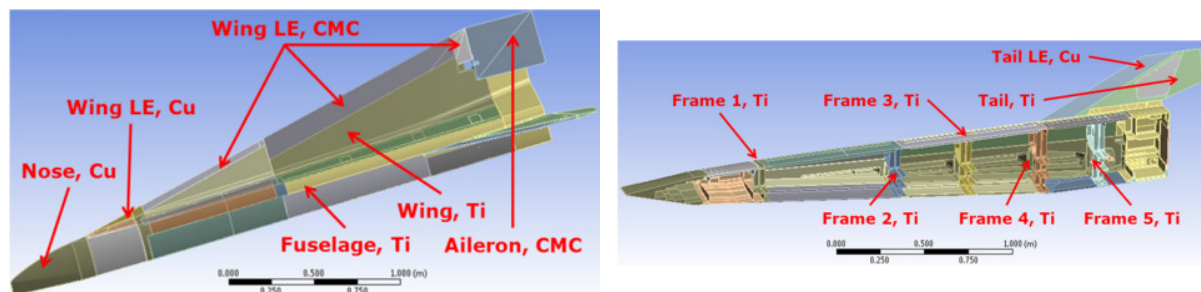**Figure 5. Main structural components of the analyzed ESM.**

Analogously, Table 3 reports the materials selected for the EFTV components highlighted in Fig. 6. In particular:
- copper for the vehicle nose;
- copper for the fore part of the wing leading edges;
- C/C-SiC for the remaining part of the wing leading edge;
- copper for the leading edge of the V-tails;
- C/C-SiC for the ailerons;
- titanium alloy for the remaining part of the structure.

In addition, as previously mentioned, a layer of 1 mm thick zirconia has been foreseen for all the metallic components. Using a conservative approach, a constant surface emissivity of 0.4, i.e. the lowest available value for zirconia, has been set for the external coated surfaces.

Table 3. Preliminarily material assignment for the main EFTV structural components

EFTV					
Nose	**Fuselage**	**Wing**	**Wing LE**	**V-Tail**	**Aileron**
Copper	Ti-Alloy	Ti-Alloy	C/C-SiC / Copper	Ti-Alloy / Copper	C/C-SiC

Figure 6. Main structural components of the analyzed EFTV.

4

American Institute of Aeronautics and Astronautics

IV. Thermal Analysis

A. Numerical Procedure

The vehicle thermal behaviour has been assessed by means of the FE method implemented in the software Ansys[12,13]. A transient thermal analysis along the computed entry path is performed to evaluate the time dependent temperature of the structure. The implemented numerical procedure is schematically reported in Fig. 7.
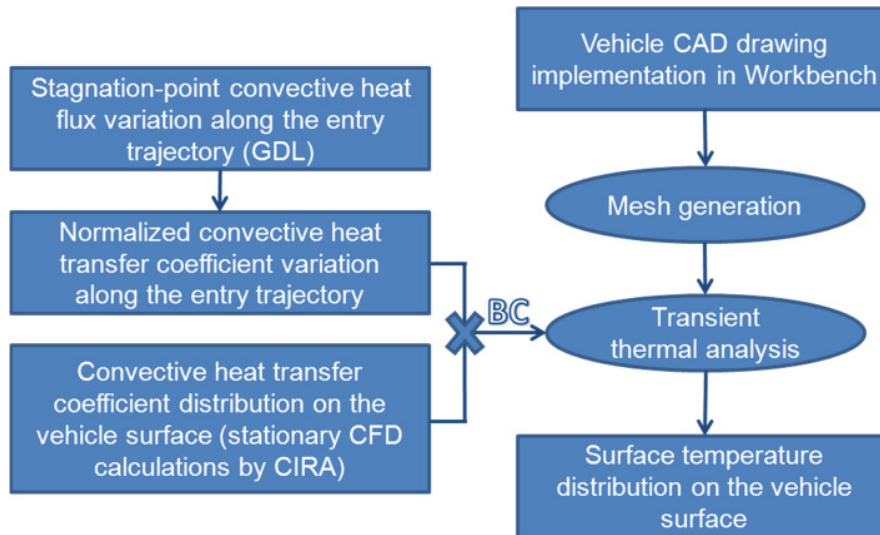
Figure 7. Numerical procedure flow chart.

In particular:
- The available CAD drawing of the vehicle is implemented in Ansys Workbench and properly modified, if required.
- The computational mesh is generated.
- Stationary CFD calculations (whose description is out of the scope of the present work) have been realized in a certain number of flight conditions to evaluate the convective heat transfer coefficient spatial distribution over the vehicle surface.
- The flight trajectory has been split in a certain number of legs, each of them characterized by a specific flight condition previously analysed by CFD (effect of angle of attack and Mach number are therefore considered, see Fig. 8a).
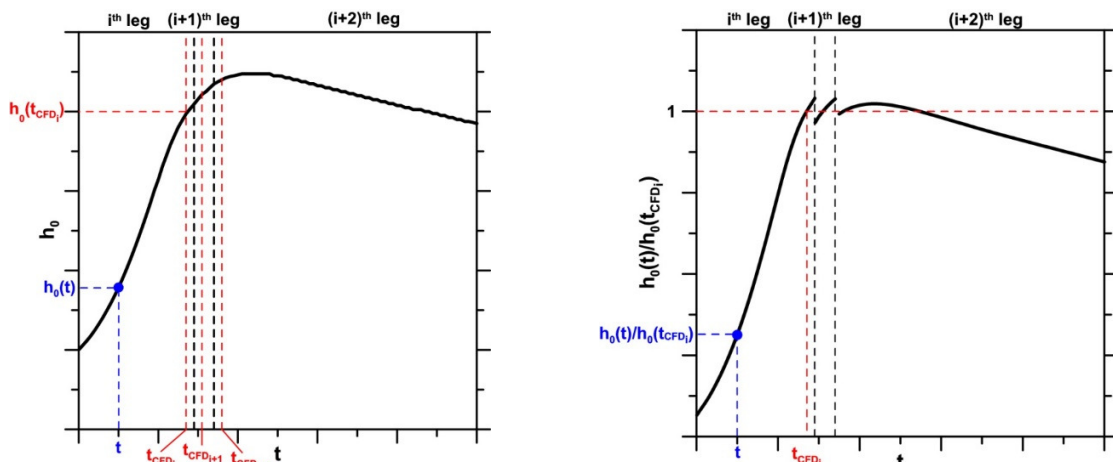
Figure 8. a) Description of CFD results scaling along the trajectory. b) Typical normalized stagnation-point heat transfer function.

5

American Institute of Aeronautics and Astronautics

- For each trajectory leg, the heat transfer coefficient distributions are properly scaled by the stagnation-point heat transfer coefficient variation along the selected trajectory leg, normalized with respect to the corresponding reference condition (i.e. the flight condition analysed by CFD). Referring to the nomenclature reported in Fig. 8a, Eq. (1) is applied.

$$h(x,t) = h(x)|_{CFD_i} \cdot \frac{h_0(t)}{h_0(t_{CFD_i})} \tag{1}$$

An exemplary plot of the normalized stagnation-point heat transfer function, piecewise-defined in each trajectory leg, is shown in Fig. 8b. In particular, the stagnation-point convective heat transfer coefficient has been estimated scaling the cold wall stagnation-point convective heat flux variation along the trajectory by the stagnation temperature profile, as reported in Eq. (2).

$$h_0 = \frac{\dot{q}_{0,cw}}{T_0} \tag{2}$$

In turn, the cold wall stagnation-point convective heat flux variation along the trajectory has been evaluated according to the Tauber's model[10].

- The transient thermal analysis is then set assuming, as convective boundary condition, the heat transfer coefficient evaluated according to the previously discussed procedure and the stagnation temperature profile (in coherence with the CFD modelling). A radiative dissipation condition is also considered for all the external surfaces. Therefore the overall condition reported in Eq. (3) is applied.

$$\dot{q} = h \cdot (T_0 - T_w) - \sigma \cdot \varepsilon \cdot T_w^4 \tag{3}$$

B. Preliminary Results

As results, according to the previously discussed method, the temporal variation of the maximum temperature on the different analysed materials and vehicle components has been plotted along the flight path. Fig. 9a reports in particular the maximum temperature variation along the flight profile on the main components of the ESM, Fig. 9b refers tp the EFTV. In Fig. 9a the starting time corresponds to the trajectory apogee, in Fig. 9b to the ESM separation.
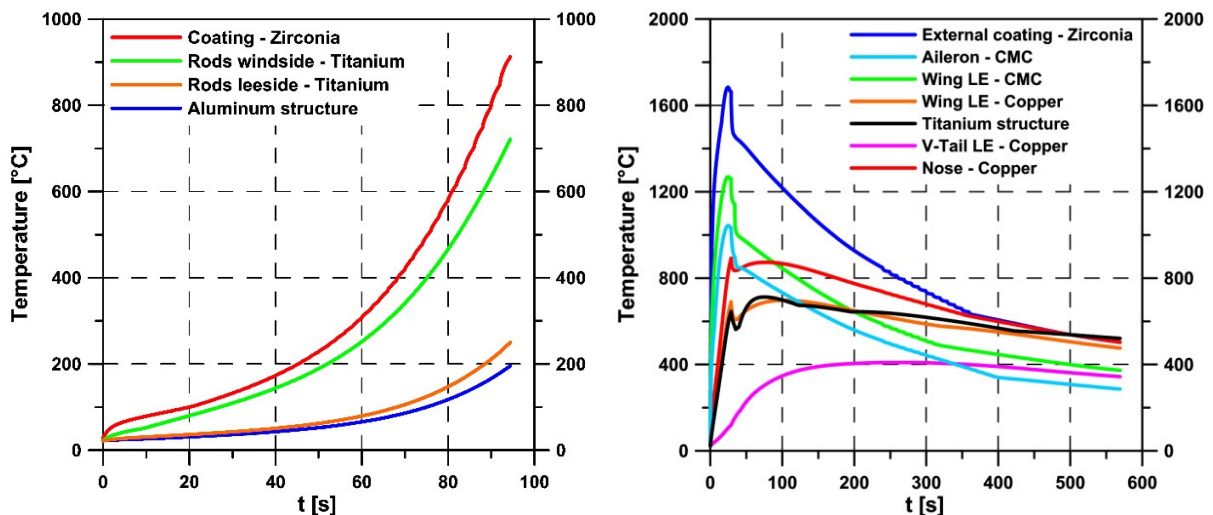
Figure 9. Maximum temperature along the flight profile on the main components a) of the ESM and b) of the EFTV

From Fig. 9a it is evdent that Titanium rods can withstand the aero-thermal loads, but a local temperature peak of about 700°C is reached at the end of the analysis for one rod. The critical temperature of 600°C is overcome for the last 4 seconds. In addition, aluminium seems to be suitable for the internal structure of the ESM.

6
American Institute of Aeronautics and Astronautics

From Fig. 9b it can be seen that zirconia coatings and C/C-SiC components (having maximum service temperatures in the order of 2400°C and 1600°C, respectively) would widely survive the aerothermal environment in these conditions. On the other hand, it can be noted that the maximum temperatures on the titanium and copper structures slightly exceed their upper working temperature limits (600 and 800°C, respectively), but only in limited spots of the vehicle, coloured in red for the titanium structure in Fig. 10. This means that such temperature overshoot can be in principle redistributed inside the vehicle structure through a future thermal structural optimization.
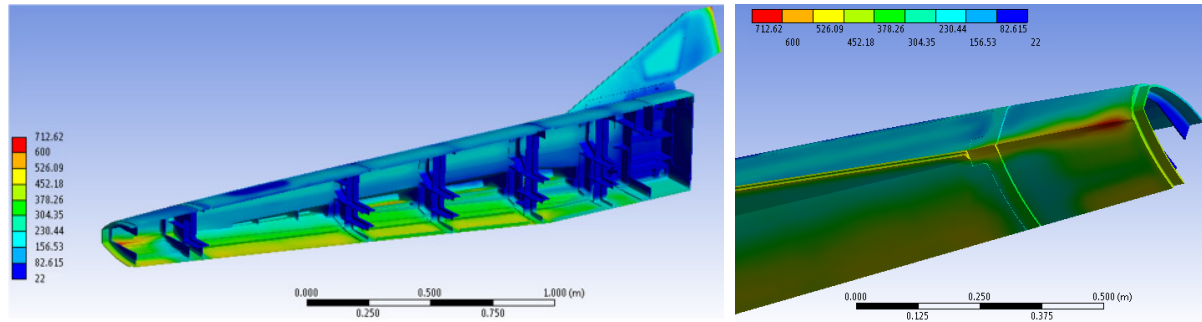
Figure 10. Temperature distribution, at the peak heating condition for titanium components of the EFTV

V. Conclusions

Finally, it can be concluded that:
- a thermal model has been realized for the structure of the EFTV and of the ESM on the basis of aero-thermal loads estimated along the flight path;
- zirconia coating guarantees a relatively large surface emissivity and a suitable thermal protection for the underlying materials;
- copper seems to be adequate for the EFTV nose and the first part of the wing leading edge, considering its ability to work as a heat sink;
- copper structures on EFTV and titanium structures both on EFTV and ESM can withstand the aerothermal environment except for limited spots, requiring a proper thermal structural optimization;
- thermal structural design is still ongoing and a numerical analysis campaign will be perform on updated structural configuration, flight trajectory and aerothermal environment.

Acknowledgments

References

[1]Steelant J., "Achievements obtained on Aero-Thermal Loaded Materials for High-Speed Atmospheric Vehicles within ATLLAS," *16th AIAA/DLR/DGLR International Space Planes and Hypersonic Systems and Technologies Conference*, AIAA-2009-7225, Bremen, Germany, 2009.

[2]Steelant, J., "Sustained Hypersonic Flight in Europe: first achievements within LAPCAT II," *17th AIAA International Space Planes and Hypersonic Systems and technologies conference*, AIAA 2011-2243, San Francisco, CA, 2011.

[3]Steelant, J., Langener, T., Hannemann, K., Marini, M., Serre, L., Bouchez, M., Falempin, F., "Conceptual Design of the High-Speed Propelled Experimental Flight Test Vehicle HEXAFLY," *20th AIAA International Space Planes and Hypersonic Systems and technologies conference*, AIAA 2015-3539, Glasgow, Scotland, 2015.

[4]Hexafly-INT Team, "Part B High-Speed Experimental Fly Vehicles–INTernational," CIRA-CF-14-1132, Italian Aerospace Research Centre (CIRA), Capua, Italy, 2014 (unpublished).

[5]Jung, W., Ettl, J., Kallenbach, A., Turner, J., "Mission Definition and System Requirements, Work Package 2.0 – Launch Vehicle," Presentation at HEXAFLY-INT MDR & SRR, Italian Aerospace Research Centre (CIRA), Capua, Italy, 2014 (unpublished).

7

American Institute of Aeronautics and Astronautics

[6]Favaloro, N., Rispoli, A., Vecchione, L., Pezzella, G., Carandente, V., Scigliano, R., Cicala, M., Morani, G., Steelant, J.. "Design Analysis of the High-Speed Experimental Flight Test Vehicle HEXAFLY-International," *20th AIAA International Space Planes and Hypersonic Systems and technologies conference*, AIAA 2015-3607, Glasgow, Scotland, 2015.

[7]Pezzella, G., Marini, M., Reimann B., Steelant, J., "Aerodynamic Design Analysis of the HEXAFLY-INT Hypersonic Glider," *20th AIAA International Space Planes and Hypersonic Systems and technologies conference*, AIAA 2015-3644, Glasgow, Scotland, 2015.

[8]Pezzella, G., van Brummen, S., Steelant, J., "Assessment of Hypersonic Aerodynamic Performance of the EFTV-ESM Configuration in the Framework of the Hexafly-INT Research Project," *8th European Symposium on Aerothermodynamics for Space Vehicles*, Lisbon, Portugal, 2015.

[9]Pezzella, G., Carandente, V., Scigliano, R., Marini, M., Steelant J., "Aerothermal Environment Methodology of the Hexafly-INT Experimental Flight Test Vehicle (EFTV)," *8th European Symposium on Aerothermodynamics for Space Vehicles*, Lisbon, Portugal, 2015.

[10]Tauber, M. E., "A review of high-speed, convective, heat-transfer computation methods," NASA Technical Paper 2914, 1989.

[11]Glass, D. E., Capriotti, D. P., Reimer, T., Kütemeyer, M., Smart, M., "Testing of DLR C/C-SiC and C/C for HIFiRE 8 Scramjet Combustor," *19th AIAA International Space Planes and Hypersonic Systems and Technologies Conference*, Atlanta, GA, 2014.

[12]ANSYS Inc., Thermal analysis guide, Release 12.1, 2009.

[13]ANSYS Inc., Structural analysis guide, Release 12.1, 2009.

8

American Institute of Aeronautics and Astronautics